Inorganic Chemistry
Cite This: Inorg. Chem. XXXX, XXX, XXX−XXX
Article
pubs.acs.org/IC

Reduction of $Ru^{VI}{\equiv}N$ to $Ru^{III}—NH_3$ by Cysteine in Aqueous Solution

Qian Wang,[†] Wai-Lun Man,[‡] William W. Y. Lam,[‡,§] Shek-Man Yiu,[‡] Man-Kit Tse,[‡] and Tai-Chu Lau*[,‡]

[†]School of Chemistry and Chemical Engineering, Shandong University of Technology, Zibo 255049, People's Republic of China
[‡]Department of Chemistry, City University of Hong Kong, Tat Chee Avenue, Kowloon Tong, Hong Kong
[§]Department of Food and Health Sciences, Technological and Higher Education Institute of Hong Kong, Tsing Yi Road, New Territories, Hong Kong

Supporting Information

ABSTRACT: The reduction of metal nitride to ammonia is a key step in biological and chemical nitrogen fixation. We report herein the facile reduction of a ruthenium(VI) nitrido complex $[(L)Ru^{VI}(N)(OH_2)]^+$ (**1**, L = *N*,*N*′-bis(salicylidene)-*o*-cyclohexyldiamine dianion) to $[(L)Ru^{III}(NH_3)(OH_2)]^+$ by L-cysteine (**Cys**), an ubiquitous biological reductant, in aqueous solution. At pH 1.0−5.3, the reaction has the following stoichiometry: $[(L)Ru^{VI}(N)(OH_2)]^+ + 3HSCH_2CH(NH_3)CO_2 \rightarrow [(L)Ru^{III}(NH_3)(OH_2)]^+ + 1.5(SCH_2CH(NH_3)CO_2)_2$. Kinetic studies show that at pH 1 the reaction consists of two phases, while at pH 5 there are three distinct phases. For all phases the rate law is rate = k_2[**1**][**Cys**]. Studies on the effects of acidity indicate that both $HSCH_2CH(NH_3^+)CO_2^-$ and $^-SCH_2CH(NH_3^+)CO_2^-$ are kinetically active species. At pH 1, the reaction is proposed to go through $[(L)Ru^{IV}(NHSCH_2CHNH_3CO_2H)(OH_2)]^{2+}$ (**2a**), $[(L)Ru^{III}(NH_2SCH_2CHNH_3CO_2H)(OH_2)]^{2+}$ (**3**), and $[(L)Ru^{IV}(NH_2)(OH_2)]^+$ (**4**) intermediates. On the other hand, at pH around 5, the proposed intermediates are $[(L)Ru^{IV}(NHSCH_2CHNH_3CO_2)(OH_2)]^+$ (**2b**) and $[(L)Ru^{IV}(NH_2)(OH_2)]^+$ (**4**). The intermediate ruthenium(IV) sulfilamido species, $[(L)Ru^{IV}(NHSCH_2CHNH_3CO_2H)(OH_2)]^{2+}$ (**2a**) and the final ruthenium(III) ammine species, $[(L)Ru^{III}(NH_3)(MeOH)]^+$ (**5**) (where H_2O was replaced by MeOH) have been isolated and characterized by various spectroscopic methods.

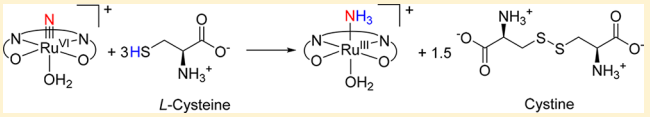

INTRODUCTION

Transition metal nitrido complexes (M≡N) and related imido complexes have received much attention in recent years because they are potentially useful reagents for nitrogenation reactions.[1−4] The reduction of metal nitride to NH_3 is also a key process in biological and chemical nitrogen fixation.[5] Among transition metal nitrido complexes, osmium(VI) nitrido complexes bearing polypyridyl or *tris*(pyrazolylborate) ligands are electrophilic and exhibit oxo-like reactivity.[6−16] Recently, a number of iron(IV) and iron(V) nitrido complexes have also been reported to display electrophilic reactivity.[17−19] Our group has shown that ruthenium(VI) nitrido complexes bearing Schiff base ligands are highly electrophilic/oxidizing. For example, $[(L)Ru^{VI}(N)(MeOH)]^+$ (**1**, L = *N*,*N*′-bis(salicylidene)-*o*-cyclohexylenediamine dianion) readily undergoes C−H bond activation of alkanes,[20] C−N bond cleavage of aniline,[21] aziridination of alkenes,[22] nitrogenation of alkynes,[23] and oxidation of phenols[24] in organic solvents.

Thiol-containing compounds play significant roles in various physiological processes, such as the protection of cells against oxidative stress, maintenance of cellular redox potentials, and regulation of metabolism and gene expression.[25−27] L-Cysteine, $HSCH_2CH(NH_3^+)CO_2^-$, is one of the simplest biological thiols. It is susceptible to oxidation by various reagents to give the corresponding disulfide (cystine), sulfenic, sulfinic, or sulfonic acids.[28] Various mechanisms have been proposed for the formation of these products, including thiol/disulfide exchange, hydrogen atom transfer, and electron transfer.[29−39] Oxidation by metal aqua species such as Fe(III) proceeds via an inner-sphere electron transfer mechanism.[31] On the other hand, oxidation by substitution-inert oxidants such as $[Ir^{IV}Cl_6]^{2-}$,[32] $[Fe^{III}(CN)_6]^{3-}$,[33] $[Fe(bpy)_2(CN)_2]^+$,[34] $[Fe(bpy)(CN)_4]^-$,[34] and $[Mo^V(CN)_8]^{3-}$[35] occurs via an outer-sphere electron transfer to produce cysteic acid, cystine, or cysteinesulfinate. More recently, a concerted electron−proton transfer (CEPT) mechanism is reported for cysteine oxidation by $M(bpy)_3^{3+}$ (M = Fe, Ru, Os) to produce $M(bpy)_3^{2+}$ and cystine.[40]

We previously reported that **1** reacts with 1 equiv of ^{t}BuSH or PhSH in CH_3CN to afford the corresponding ruthenium(IV) sulfilamido species.[41] The lack of RSH/RSD deuterium isotope effects suggests that the reaction occurs via a rate-limiting nucleophilic attack of RSH at **1** followed by a fast proton shift. We report herein the facile reduction of **1** by L-cysteine to $[(L)Ru^{III}(NH_3)(OH_2)]^+$ in aqueous acidic solutions (Scheme 1). In this case, kinetic and mechanistic studies suggest that proton-coupled electron transfer processes are involved in the reaction. Although there is an extensive aqueous redox chemistry of metal−oxo species, corresponding aqueous metal nitrido chemistry has received much less attention.[42−44]

EXPERIMENTAL SECTION

Materials. $[(L)Ru^{VI}(N)(MeOH)](ClO_4)$ was prepared by a literature method.[45] L-Cysteine (Aldrich, ≥97.0%), CF_3CO_2H

Received: January 27, 2018

DOI: 10.1021/acs.inorgchem.8b00238
Inorg. Chem. XXXX, XXX, XXX−XXX

Scheme 1. Reaction of 1 with Cys in Aqueous Solutions at Different pH Values

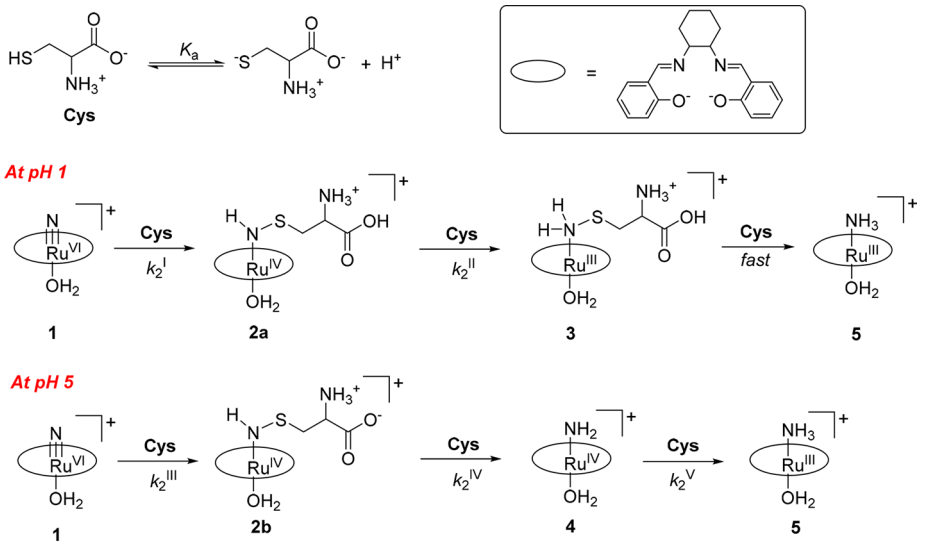

(Aldrich, ≥99.0%), CF_3CO_2D (Aldrich, ≥99.0%), CH_3CO_2Na (Aldrich, ≥99.0%), CH_3CO_2H (Aldrich, 99.8%), D_2O (Cambridge Isotope, 99.8 atom % D), and DMSO (Aldrich, ≥99.0%) were used as received. The deuterated cysteine, $DO_2CCH(ND_2)CH_2SD$, was prepared by recrystallization from D_2O and characterized by Raman spectroscopy.[46] Water for kinetic experiments was distilled twice from alkaline permanganate. All other chemicals were of reagent grade and were used without further purification. Ionic strength was maintained with CF_3CO_2Na (Aldrich, 98%). The pH values of solutions were determined either by direct titration with standard NaOH solutions or by using a pH meter (Mettler Toledo, FE 20). For D_2O solutions, the pD values were obtained from a pH meter using the relationship pD = pH_{meas} + 0.4.

Instrumentation. The kinetics of the reaction were studied by using either an Agilent 8453 diode−array spectrophotometer or an Applied Photophysics SX20 stopped-flow spectrophotometer. The temperature of the solutions was maintained with a PolyScience digital temperature controller connected to a circulating water bath. Electrospray ionization mass spectrometry (ESI/MS) was done on an API 150EX mass spectrometer. The analyte solution was continuously infused with a syringe pump at a constant flow rate of 10 μL min^{-1} into the pneumatically assisted electrospray probe with nitrogen as the nebulizing gas. The declustering potential was typically set at 10 V. NMR spectra were recorded ona Bruker (600 MHz) FT-NMR spectrometer.

Kinetics. The concentrations of cysteine were at least in 10-fold excess of that of **1**. The reaction progress was monitored by observing absorbance changes at 551 nm for the first and second phases at pH < 3. At pH > 4.5, the kinetics of the reaction were monitored at 551 nm for the first phase and at 519 nm for the second and third phases. Pseudo-first-order rate constants, k_{obs}, were obtained by nonlinear least-squares fits of A_t versus time t according to the equation $A_t = A_\infty + (A_0 - A_\infty)\exp(-k_{obs}t)$, where A_0 and A_∞ are the initial and final absorbance, respectively.[47]

Product Analysis. The ruthenium product for the reduction of **1** by **Cys** was detected by the following procedure. **Cys** (1.06×10^{-3} M) was allowed to react with **1** (1.06×10^{-4} M) in 1 mM CF_3CO_2H (2 mL) at 25 °C. The resulting solution was analyzed by ESI/MS at various time intervals.

The organic products were detected by ^1H NMR. In a typical reaction, a mixture containing **Cys** (1.71×10^{-2} mmol) and **1** (2.85×10^{-3} mmol) in 1 mL of 1 mM CF_3CO_2D in D_2O was stirred at 25 °C under argon. After 12 h, 77 μL of CF_3CO_2D was added to dissolve the precipitated cystine. DMSO (1.32×10^{-3} M) was added as internal standard, and the mixture was analyzed by ^1H NMR.

Synthesis of $[(L)Ru^{IV}(NHSCH_2CHNH_3CO_2H)(OH_2)](ClO_4)_2 \cdot 2H_2O \cdot 0.3EtOH$ (2a[ClO_4]$_2$). A solution of cysteine (12.1 mg, 0.1 mmol) in 0.1 M $HClO_4$ (83.3 μL) was slowly added to an orange solution of $[(L)Ru^{VI}(N)(MeOH)](ClO_4)$ (56.7 mg, 0.1 mmol) in EtOH (8 mL) containing $HClO_4$ (48 μL), and the mixture was stirred in an ice bath for 20 min. The resulting deep-purple solution was filtered and followed by the addition of diethyl ether (200 mL). The resulting purple precipitate was filtered off and washed by CH_2Cl_2 and Et_2O. The solid was recrystallized from EtOH/Et_2O and dried in vacuo at room temperature. Yield: 63%. ^1H NMR (600 MHz) in CD_3OD (0.5 mL)/$HClO_4$ (1 μL): δ 8.71 (s, 1H, N = CH), 8.67 (s, 1H, N = CH), 7.56−7.64 (m, 2H), 7.42−7.46 (m, 2H), 6.82−6.84 (t, 2H), 4.42 (s, 1H, N−CH), 4.18−4.21 (t, 1H, N−CH), 3.99−4.05 (tt, 1H, C*H*CO_2H), 3.48−3.63 (m, 2H, S−CH), 3.25−3.28 (m, 2H), 2.02−2.25 (m, 4H), 1.72−1.80 (m, 2H), 1.30 (s, 1H, CO_2H). ^{13}C NMR (151 MHz) in CD_3OD (0.5 mL)/$HClO_4$ (1 μL): 49.41 (SCH_2CO_2H), 45.48 (SCH_2CO_2H). Elem. anal.: Calcd (%) for $C_{23}H_{30}Cl_2N_4O_{13}RuS \cdot 2H_2O \cdot 0.3EtOH$: C, 34.38; H, 4.38; N, 6.80. Found: C, 34.13; H, 4.63; N, 6.79. UV/vis (in 0.1 M CF_3CO_2H): λ_{max}[nm] (ε[mol^{-1} dm^3 cm^{-1}]): 552 (3900), 374 (10600), 339 (14400). ESI/MS in EtOH (1 mL)/$HClO_4$ (1 μL): *m*/*z* 557 {[(L)Ru($NHSCH_2CHNH_3CO_2$)]$^+$}, 603 {[(L)Ru($NHSCH_2CHNH_3CO_2$)-(EtOH)]$^+$}.

Synthesis of $[(L)Ru^{III}(NH_3)(MeOH)](ClO_4) \cdot MeOH$ (5[ClO_4]). A solution of cysteine (12.1 mg, 0.1 mmol) in 0.1 M $HClO_4$ (83.3 μL) was slowly added to a purple solution of **2a** (42 mg, 0.05 mmol) in MeOH (2 mL) containing $HClO_4$ (20 μL), and the mixture was stirred for 3 h. The resulting dark green solution was filtered and slow evaporation of the filtrate gave dark green single crystals that are suitable for X-ray analysis. Yield: 70%. IR (KBr, cm^{-1}): ν(N−H) 3321(s), 3236(w), 3134(s). Elem. anal.: Calcd (%) for $C_{21}H_{27}ClN_3O_7Ru \cdot MeOH$: C, 43.89; H, 5.19; N, 6.98. Found: C, 43.77; H, 5.28; N, 6.99. UV/vis (in 0.1 M CF_3CO_2H): λ_{max}[nm] (ε[mol^{-1} dm^3 cm^{-1}]): 628 (4040), 374 (16200), 351 (14800), 231 (35800). ESI/MS in MeOH: *m*/*z* 439 {[(L)Ru(NH_3)]$^+$}, 471 {(L)[Ru(NH_3)(MeOH)]$^+$}.

X-ray Crystallography. A crystal of dimensions 0.39 × 0.09 × 0.02 mm coated with paratone-N and mounted on a nylon cryoloop was used for X-ray diffraction analysis. X-ray diffraction data of 5[ClO_4] were collected using ω-scan mode at 193 K on an Oxford Diffraction Gemini S Ultra 4-circle kappa diffractometer with a 92 mm diagonal Sapphire CCD detector using monochromatized Cu-Kα radiation (λ = 1.5418 Å). Details of the intensity data collection and crystal data are given in Table S1. The data were processed and absorption correction was done by multiscan method using CrysAlis.[48] The structure was solved and refined using full-matrix least-squares

DOI: 10.1021/acs.inorgchem.8b00238
Inorg. Chem. XXXX, XXX, XXX−XXX

based on F^2 with programs SHELXS-97[49] and SHELXL-97[49] within Olex2.[50] Ruthenium and many nonhydrogen atoms were located according to the direct method. The positions of other nonhydrogen atoms were found after successful refinement using program SHELXL-97. In the final stage of refinement, all nonhydrogen atoms were refined anisotropically. H atoms were generated by program SHELXL-97. The positions of H atoms were calculated based on riding model with thermal parameters equal to 1.2 times (1.5 times for H atoms in methyl groups) that of the associated C atoms and N atoms, and these are participated in the calculation of final *R*-indices.

Warning. Although we have not encountered any explosions so far, perchlorate salts of ruthenium complexes should be handled with extreme caution and in quantities not greater than 100 mg.

RESULTS AND DISCUSSION

Spectrophotometric Changes. Rapid spectrophotometric changes were observed when **1** was mixed with excess **Cys** in aqueous acidic solution under argon. Repetitive scanning at different time scales indicates that the reaction occurs in two distinct phases at pH < 3. The spectral changes at pH = 1 are shown in Figure 1. Well-defined isosbestic points are

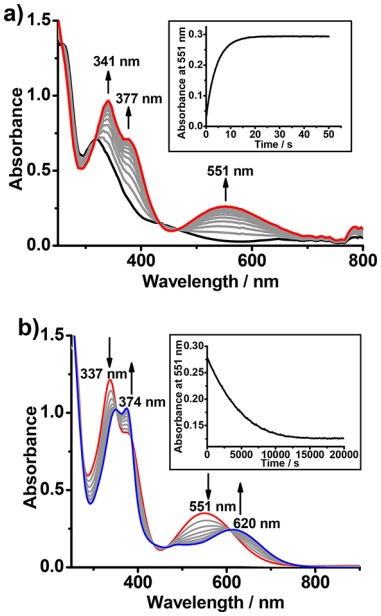

Figure 1. Spectral changes for the reaction of **1** (6.69×10^{-5} M) with **Cys** (6.69×10^{-4} M) in 0.1 M CF_3CO_2H at 25.0 °C, I = 0.1 M. (a) Spectra collected at 1 s intervals using a stopped-flow spectrophotometer, showing the first phase. (b) Spectra collected at 960 s intervals using a diode-array spectrophotometer, showing the second phase of the reaction. Insets show the corresponding time traces at 551 nm.

maintained at 257, 316, 433, and 467 nm for the first phase and at 259, 351, 385, 432, 464, and 605 nm for the second phase. At pH > 4.5, the reaction is much faster, and in this case, three distinct phases were observed; the spectral changes at pH = 5.3 are shown in Figure 2. Well-defined isosbestic points are maintained at 316 nm for the first phase, at 452 nm for the second phase, and at 359 nm for the third phase.

Kinetics. The kinetics of the reaction were followed at 551 nm for both the first and second phase at pH < 3. In the presence of at least 10-fold excess of **Cys**, clean pseudo-first-order kinetics were observed for over three half-lives (Figure 1, insets). The pseudo-first-order rate constants, k_{obs}, depend linearly on [**Cys**] (Figure 3). The second-order rate constants

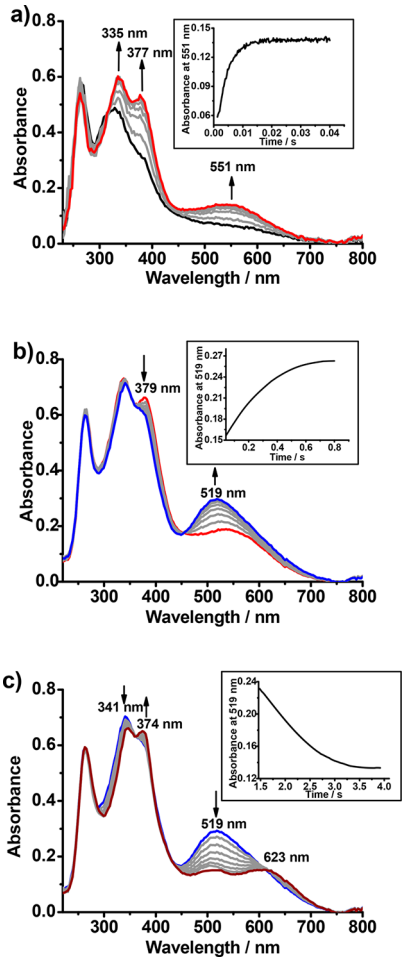

Figure 2. Spectral changes for the reaction of **1** (4.08×10^{-5} M) with **Cys** (5.00×10^{-4} M) at 25.0 °C, pH = 5.30, and I = 0.1 M. Data were obtained using a stopped-flow spectrophotometer. (a) Spectra collected at 0.002 s intervals showing the first phase. (b) Spectra collected at 0.1 s intervals showing the second phase. (c) Spectra collected at 0.35 s intervals showing the third phase of reaction. Insets show the corresponding time traces.

for the first (k_2^{I}) and second (k_2^{II}) phases are determined to be $(4.10 \pm 0.05) \times 10^2$ and $(8.73 \pm 0.20) \times 10^{-2}$ M^{-1} s^{-1} at 25.0 °C, pH = 1.00, and I = 0.1 M, respectively.

At pH > 4.5, three phases were observed. The kinetics of the reaction were monitored at 551 nm for the first phase and 519 nm for the second and third phase. The pseudo-first-order rate constants, k_{obs}, depend linearly on [**Cys**] for all three phases (Figure 4). The second-order rate constants for the first (k_2^{III}), second (k_2^{IV}), and third (k_2^{V}) phases were determined to be $(5.19 \pm 0.09) \times 10^5$, $(1.84 \pm 0.07) \times 10^2$, and $(5.07 \pm 0.15) \times 10^1$ M^{-1} s^{-1}, respectively, at 25.0 °C, pH = 5.30, and I = 0.1 M. The nonzero intercepts in the plots for the second and third phases are probably due to background decomposition of the ruthenium(IV) intermediate (see SI and below).

Effects of Acidity. The effects of acidity on k_2 for the first phase were studied over the pH range of 1.00−5.30. Representative data are summarized in Table S2. The plot of k_2 vs pH is shown in Figure 5; such a kinetic behavior is consistent with the rate law shown in eq 1.

$$k_2 = \frac{k_a[H^+] + k_b K_a}{[H^+] + K_a} \quad (1)$$

DOI: 10.1021/acs.inorgchem.8b00238
Inorg. Chem. XXXX, XXX, XXX−XXX

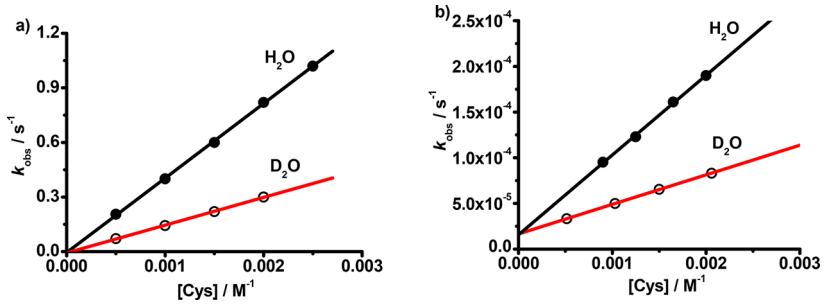

Figure 3. Plot of k_{obs} vs [**Cys**] for the reaction of **1** with **Cys** at 25.0 °C, pH (or pD) = 1.00 and I = 0.1 M: (a) first phase; (b) second phase.

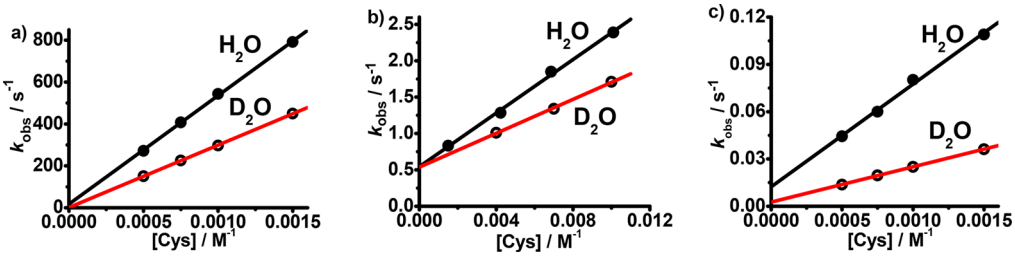

Figure 4. Plot of k_{obs} vs [**Cys**] for the reaction of **1** with **Cys** at 25.0 °C, pH (or pD) = 5.30, and I = 0.1 M: (a) first phase, (b) second phase, and (c) third phase.

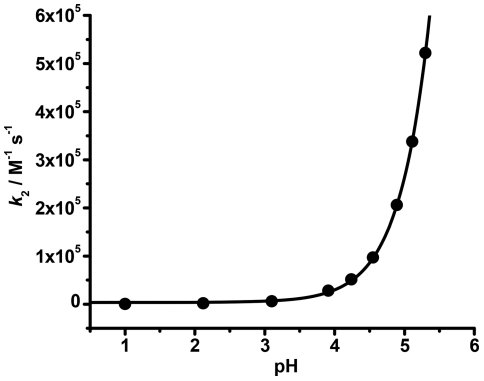

Figure 5. Plot of k_2 vs pH for the first phase of the oxidation of **Cys** by **1** at 25.0 °C and I = 0.1 M.

K_a is the acid dissociation constant of the S−H of L-cysteine and is taken as 4.27×10^{-9} M.[51] k_a and k_b are the rate constants for oxidation of $HSCH_2CH(NH_3^+)CO_2^-$ and $^-SCH_2CH(NH_3^+)CO_2^-$, respectively. A nonlinear least-squares fit of the data to eq 1 gives $k_a = (4.01 \pm 1.03) \times 10^3$ M^{-1} s^{-1} and $k_b = (6.07 \pm 0.03) \times 10^8$ M^{-1} s^{-1} at 25.0 °C and I = 0.1 M.

Kinetic Isotope Effects. The kinetics were also investigated in D_2O at pD = 1.0 and 5.3 at 25.0 °C (Figure 3 and Figure 4) and the data are summarized in Table 1. At pH (or pD) = 1.00, the kinetic isotope effects (KIEs) for the first and the second phase are the same, $k_2^{I}(H_2O)/k_2^{I}(D_2O) = k_2^{II}(H_2O)/k_2^{II}(D_2O) = 2.7$. On the other hand, at pH = 5.30, the KIEs for the first, second, and third phases are $k_2^{III}(H_2O)/k_2^{III}(D_2O) = 1.7$, $k_2^{IV}(H_2O)/k_2^{IV}(D_2O) = 1.6$, and $k_2^{V}(H_2O)/k_2^{V}(D_2O) = 2.3$.

Activation Parameters. The effects of temperature on the rate constants were studied from 288 to 318 K at I = 0.1 M (Tables S3−S5 and Figures S1−S4). Activation parameters were obtained from the plot of $\ln(k_2/T)$ versus $1/T$ according to the Eyring equation and the data are summarized in Table 1.

Product Analysis. The ruthenium intermediates and product for the reaction of **1** with 10 equiv of **Cys** at pH 3 were examined by electrospray ionization mass spectrophotometry (ESI/MS). The solution turned from orange to purple immediately after mixing, and a predominant peak at m/z = 557 was observed in the mass spectrum, which is assigned as a ruthenium sulfilamido species, $[(L)Ru(NHSCH_2CHNH_3CO_2)]^+$ (Figure 6a). The relative intensity of the m/z 557 peak gradually decreased, with concomitant appearance of a new peak at one mass unit higher (m/z 558), which is assigned to $[(L)Ru(NH_2SCH_2CHNH_3CO_2)]^+$. Minor peaks at m/z 439 $\{[(L)Ru(NH_3)]^+\}$ and 457 $\{[(L)Ru(NH_3)(OH_2)]^+\}$ also gradually appeared, as shown in Figure 6b. After

Table 1. Kinetic Data for the Oxidation of Cys by 1 at Various pHs

pH	k_2 (M^{-1} s^{-1} at 25.0 °C)	KIE	$\Delta H^{‡}$ (kcal mol^{-1})	$\Delta S^{‡}$ (cal mol^{-1}·K^{-1})
1.00	$(4.20 \pm 0.05) \times 10^{2a}$	2.7[a]	$(6.7 \pm 0.4)^a$	$-(24 \pm 1)^a$
	$(8.73 \pm 0.20) \times 10^{-2b}$	2.7[b]	$(1.7 \pm 0.1) \times 10^{1b}$	$-(6 \pm 1)^b$
4.88	$(2.00 \pm 0.07) \times 10^{5a}$		$(8.9 \pm 0.4)^a$	$-(5 \pm 1)^a$
	$(1.59 \pm 0.05) \times 10^{2b}$		$(1.4 \pm 0.1) \times 10^{1b}$	$-(1 \pm 1)^b$
	$(4.10 \pm 0.20) \times 10^{1c}$		$(1.5 \pm 0.1) \times 10^{1c}$	$-(1 \pm 1)^c$
5.30	$(5.19 \pm 0.09) \times 10^{5a}$	1.7[a]		
	$(1.84 \pm 0.07) \times 10^{2b}$	1.6[b]		
	$(5.07 \pm 0.15) \times 10^{1c}$	2.3[c]		

[a]First phase. [b]Second phase. [c]Third phase.

DOI: 10.1021/acs.inorgchem.8b00238
Inorg. Chem. XXXX, XXX, XXX−XXX

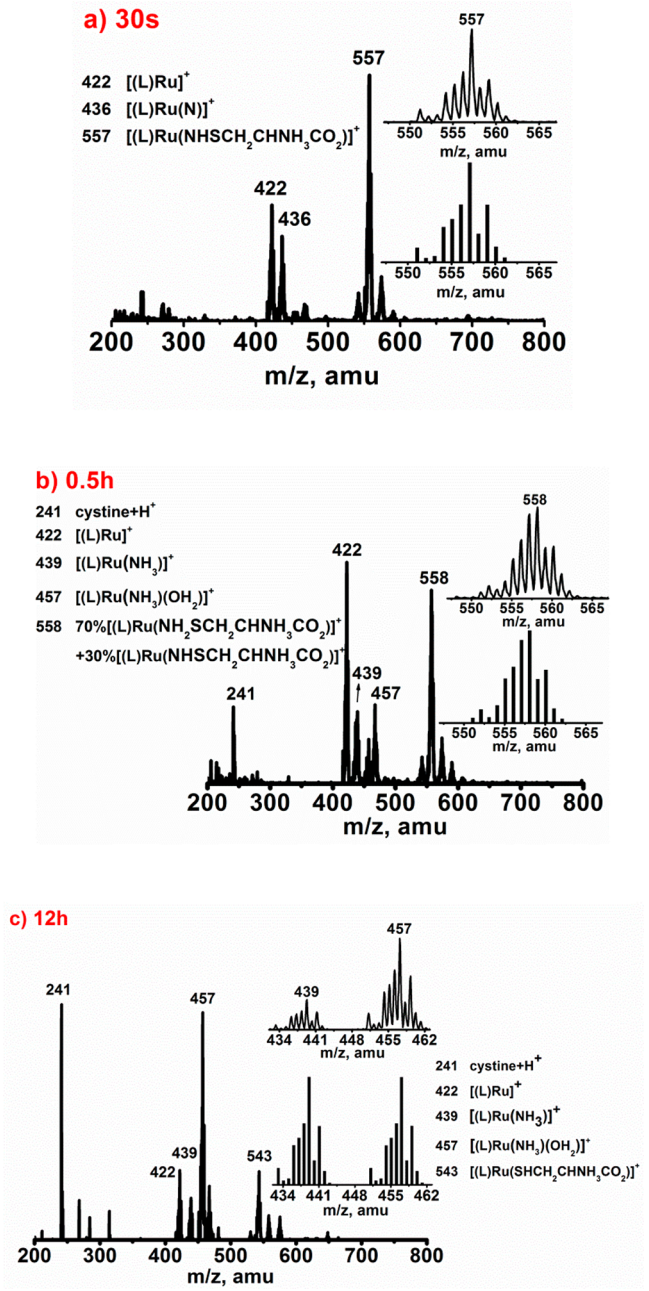

Figure 6. ESI/MS (+ve mode) of the reaction mixture of **1** (1.06×10^{-4} M) and **Cys** (1.06×10^{-3} M) in 1 mM CF_3CO_2H taken at various time intervals. Insets show expanded (top) and simulated (bottom) isotopic distribution patterns.

12 h, the m/z 457 peak became predominant (Figure 6c). In addition, the peak at m/z = 241 increased as the reaction progressed, which is assigned to the protonated cystine, {[cystine + H]$^+$}.

The protonated cystine product detected by ESI/MS was further analyzed by ^{1}H NMR (see experimental section). **1** (2.85×10^{-3} mmol) was reacted with 6 equiv of **Cys** (1.71×10^{-2} mmol) in 1 mM CF_3CO_2D in D_2O. After 12 h, the ^{1}H NMR spectrum (Figure 7) exhibits two sets of protons arising from **Cys** (δ 4.16, 2.97, 2.92 ppm) and cystine (δ 4.29, 3.25, 3.09 ppm). The amount of cystine produced and **Cys** remained are determined to be $(3.95 \pm 0.02) \times 10^{-3}$ M (ca. 1.5 equiv) and $(8.29 \pm 0.04) \times 10^{-3}$ M (ca. 3 equiv), respectively, using DMSO as the internal standard. The ^{1}H NMR and the MS results together reveal that the overall stoichiometry for the reaction of **1** with **Cys** is as shown in eq 2.

$$[(L)Ru^{VI}(N)(OH_2)]^+ + 3HSCH_2CH(NH_3)CO_2 \rightarrow [(L)Ru^{III}(NH_3)(H_2O)]^+ + 1.5O_2C(NH_3)CHCH_2S{-}SCH_2CH(NH_3)CO_2 \quad (2)$$

Isolation of Ruthenium Intermediate and Product. The ruthenium sulfilamido intermediate, which was detected by ESI/MS, has been isolated as the ClO_4^- salt, $[(L)Ru^{IV}(NHSCH_2CHNH_3CO_2H)(OH_2)](ClO_4)_2$ (**2a**$[ClO_4]_2$), from the reaction of **1** with 1 equiv of **Cys** in EtOH/$HClO_4$ solution. Similar purple sulfilamido complexes $[(L)Ru^{IV}(NHSR)(NCCH_3)]^+$ (R = ^{t}Bu or Ph), prepared from the reaction of **1** with 1 equiv of RSH in CH_3CN, have been reported.[41] Complex **2a** is diamagnetic and its NMR spectra are consistent with N−S bond formation. For example, the ^{1}H NMR spectrum (Figure S5) reveals that the two imine protons of the salen occur as two singlets at δ 8.67 and 8.71 ppm. With the support of its ^{1}H−^{1}H COSY spectrum (Figure S6), the α-CH and two β-CHs of the sulfilamido ligand are assigned as two sets of triplet (δ 3.95−4.26 ppm) and a multiplet (δ 3.50−3.68 ppm), respectively. The ^{13}C NMR spectrum (Figure S7) indicates that the β-C atom of sulfilamido ligand is located at 45.48 ppm, which is shifted from 24.06 ppm of the free cysteine. This ^{13}C assignment is further confirmed by ^{13}C−^{1}H HSQC experiments (Figure S8). The IR spectrum of **2a** shows that the N atom is protonated rather than the S atom. A ν(N−H) stretching band occurs at 3219 cm^{-1}, which is higher than the ν(N−H) stretches of cysteine at 3178 and 2963 cm^{-1} (Figure S9); while no υ(S−H) stretch around 2550 cm^{-1} can be detected. The ESI/MS spectrum (Figure S10) shows peaks at m/z 557 {[(L)Ru(NHSCH$_2$CHNH$_3$CO$_2$)]$^+$} and 603 {[(L)Ru(NHSCH$_2$CHNH$_3$CO$_2$)(EtOH)]$^+$}.

The ruthenium ammine product, which was detected by ESI/MS, has been isolated as $[(L)Ru^{III}(NH_3)(MeOH)](ClO_4)\cdot MeOH$ (**5**$[ClO_4]$) by carrying out the reaction of **2a** with excess **Cys** in MeOH. Its UV/vis spectrum in 0.1 M CF_3CO_2H is similar to the final spectrum of reaction mixture of excess **Cys** with **2a** (Figure S13). The molecular structure has been determined by X-ray crystallography (Figure 8). The Ru atom is octahedrally coordinated by a tetradentate salen ligand on the plane, one NH_3 and one MeOH ligand at the apical position. The Ru−N(NH_3) bond distance of 2.073(3) Å is similar to those of 2.083(4) and 2.104(2) Å in $[(L)Ru^{III}(NH_3)(NCCH_3)]^+$ and $[(L)Ru^{III}(NH_3)(pyridine)]^+$, respectively.[41,51] ESI/MS of this complex shows peaks at m/z 471 {[(L)Ru^{III}(NH$_3$)(MeOH)]$^+$} and m/z 439 {[(L)Ru^{III}(NH$_3$)]$^+$} (Figure S14), which is comparable to those final ruthenium products of {[(L)Ru^{III}(NH$_3$)(OH$_2$)]$^+$} (m/z = 457) and {[(L)Ru^{III}(NH$_3$)]$^+$} (m/z = 439) obtained in Figure 6c.

Proposed Mechanism. L-Cysteine can potentially undergo nucleophilic attack at **1** via the N, O or S atoms. However, since there is no reaction between **1** and 20 equiv of glycine (NH_2-CH_2-COOH) for 24 h at room temperature in aqueous acidic solutions, we conclude that only the thiol group of **Cys** reacts with **1**.

In aqueous solutions, the ionization of cysteine can be described by eq 3.[52]

In aqueous acidic solutions, the observed pH dependence of k_2 on the first phase of the reaction is consistent with parallel

DOI: 10.1021/acs.inorgchem.8b00238
Inorg. Chem. XXXX, XXX, XXX−XXX

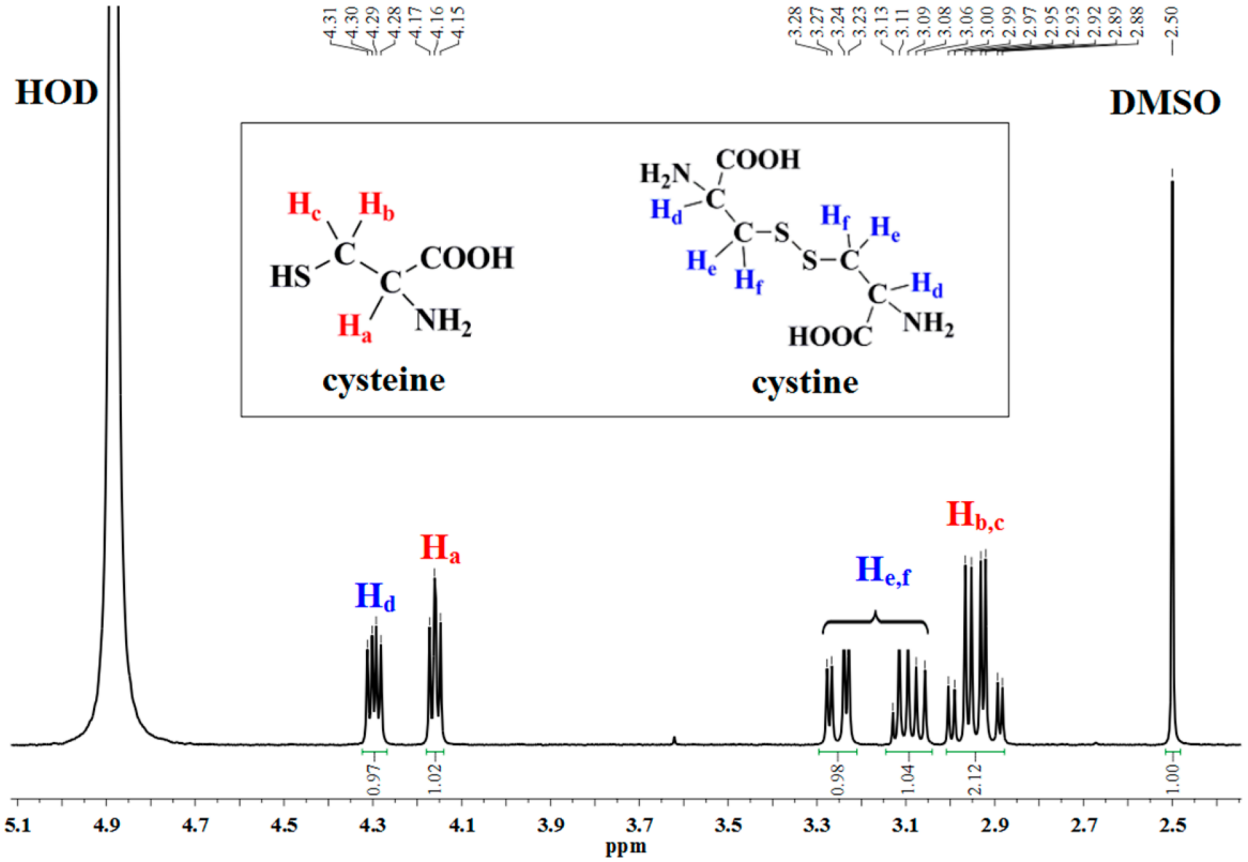

Figure 7. ^{1}H NMR spectrum of the product solution of **1** with 6 equiv of **Cys** in 1 mM CF_3CO_2D in D_2O.

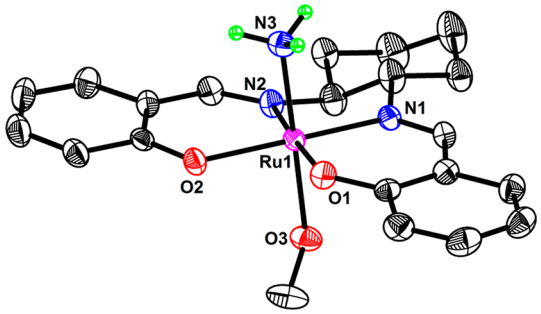

Figure 8. Molecular structure of the cation of $[(L)Ru^{III}(NH_3)(MeOH)](ClO_4)$. Thermal ellipsoids are drawn at 50% probability. H atoms [except N(3)−H] are omitted for clarity.

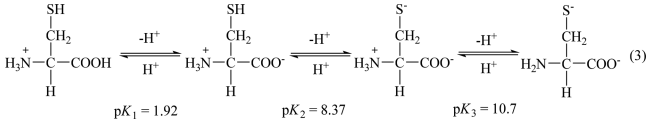

pathways involving the nucleophilic addition of $HSCH_2CH(NH_3^+)CO_2^-$ and $^-SCH_2CH(NH_3^+)CO_2^-$ to the nitrido ligand, resulting in N−S bond formation (Scheme 2).

The final UV/vis spectrum for the first phase is similar to that of isolated ruthenium(IV) sulfilamido complex complex **2a** (Figure S11).

At pH = 1, the k_a pathway predominates, and a solvent KIE of 2.7 suggests that the formation of the ruthenium(IV) sulfilamido species involves O−H cleavage in the rate-limiting step. In our previous work on the oxidation of SO_3H^- by **1**, we proposed a mechanism that involves concerted N−S bond

Scheme 2. Proposed Mechanism for the First Phase of the Reaction of 1 with Cys

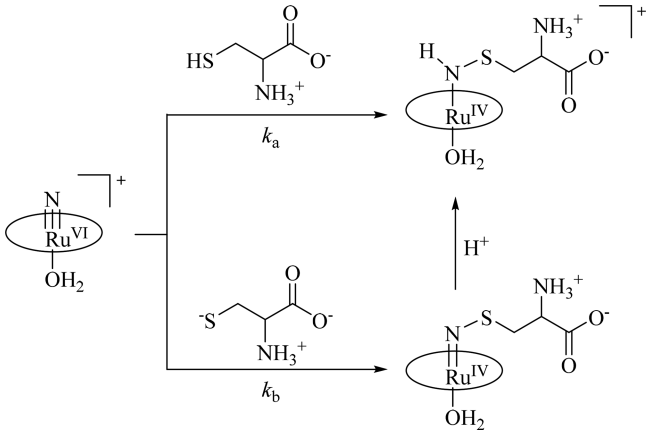

formation and proton transfer from SO_3H^- to a neighboring H_2O.[44] In this reaction, we propose a similar mechanism for the k_a pathway, that is, both N−S bond formation between **1** and **Cys** and proton transfer from **Cys** to a neighboring H_2O molecule occurs in the rate-limiting step (eq 4). The rather negative $\Delta S^{\ddagger}$ value of −24 cal mol^{-1} K^{-1} suggests an ordered transition state, which is consistent with this mechanism.

For the k_b pathway, it is proposed that the ruthenium(IV) sulfilamido species is formed via direct nucleophilic attack of the thiolate group at **1** followed by rapid protonation by the solvent (eq 5). The observed small kinetic isotope effect of 1.7 at pH = 5.3, which probably arises from the acid/base

DOI: 10.1021/acs.inorgchem.8b00238
Inorg. Chem. XXXX, XXX, XXX−XXX

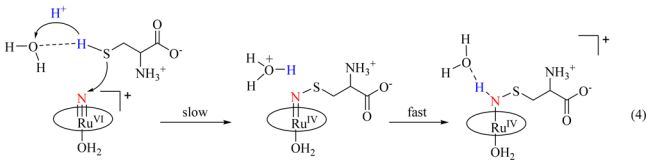

(4)

equilibrium of cysteine shown in eq 3, is consistent with this mechanism.

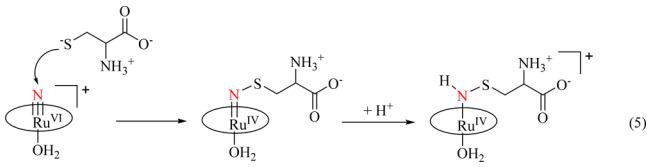
(5)

The proposed mechanism for the phase two of the reaction at pH < 3 is represented by eqs 6, 7, and 8. The first step (eq 6)

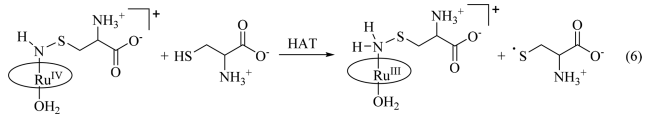

(6)

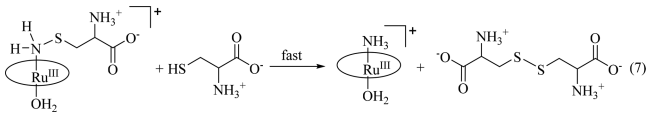

(7)

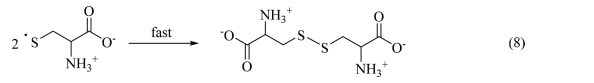

(8)

involves rate-limiting hydrogen-atom transfer (HAT) from $HSCH_2CHNH_3CO_2$ to the ruthenium(IV) sulfilamido complex $[(L)Ru^{IV}(NHSCH_2CHNH_3CO_2)]^+$ to give the ruthenium(III) sulfilamine complex $[(L)Ru^{III}(NH_2SCH_2CHNH_3CO_2)]^+$ and $^{\bullet}SCH_2CHNH_3CO_2$; the latter radical species rapidly couple to give cystine (eq 8). The HAT mechanism is supported by a KIE of 2.7 (at pH 1). The ruthenium(III) sulfilamine species could be detected by ESI/MS (Figure 6). $[(L)Ru^{III}(NH_2SCH_2CHNH_3CO_2)]^+$ then reacts rapidly with another molecule of cysteine to give the final ruthenium product, $[(L)Ru^{III}(NH_3)]^+$, together with one molecule of cystine (eq 7). Since this step occurs after the rate-limiting step, no mechanistic information could be obtained. We speculate that this step occurs via initial homolytic N−S cleavage to give a ruthenium(IV) amido species, $[(L)Ru^{IV}(NH_2)]^+$ (eq 9), followed by HAT from another **Cys** molecule to give ruthenium(III) amine (eq 10).

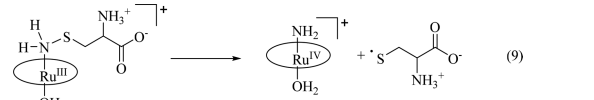
(9)

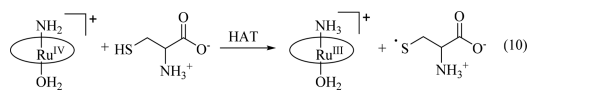

(10)

We have also monitored the reduction of **2a** by **Cys** at pH 1 independently. Upon mixing **2a** with excess **Cys** in 0.1 M CF_3CO_2H, the UV/vis spectral changes (Figure S12) are similar to those of the second phase of the reaction between **1** and **Cys** (Figure 1), and the final spectrum is very similar to that of **5** (Figure S13).

At pH > around 5, $[(L)Ru^{IV}(NHSCH_2CHNH_3CO_2)]^+$ is reduced to $[(L)Ru^{III}(NH_3)]^+$ via two kinetically distinct (second and third) phases. We propose that the second phase involves nucleophilic attack at the S-atom of ruthenium(IV) sulfilamido species by a deprotonated **Cys** with concomitant N−S cleavage, this is followed by rapid protonation to produce a ruthenium(IV) amido species $[(L)Ru^{IV}(NH_2)]^+$ and cystine (eq 11). The observed small

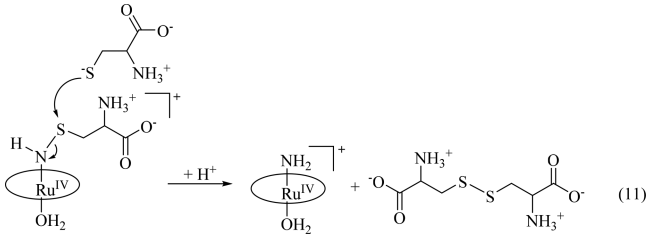
(11)

KIE of 1.6 at pH 5.3 is consistent with this mechanism. In the third phase HAT occurs from a cysteine molecule to $[(L)Ru^{IV}(NH_2)]^+$ to give the $[(L)Ru^{III}(NH_3)]^+$ product and a $^{\bullet}SCH_2CHNH_3CO_2$ radical (eq 10); the latter species rapidly dimerizes to form cystine (eq 8). The observed second-order rate law and the significant deuterium isotope effects (>2) for the third phase is consistent with a HAT mechanism. This step (eq 10) is also proposed for reaction at pH < 3 but was not observed because it is much faster than the phase one step at pH < 3.

CONCLUSIONS

In conclusion, we have reported the first example of the reduction of a metal nitrido species by L-cysteine in aqueous solution. The electrophilic ruthenium(VI) nitrido complex is rapidly and cleanly reduced by L-cysteine to ruthenium(III) ammine via ruthenium(IV) sulfilamido, ruthenium(III) sulfilamine, and ruthenium(IV) amido intermediates. Our results also reveal an interesting solvent effect on the nucleophilic addition of thiol to **1**. In CH_3CN, no S−H/S−D isotopic effects were observed in the reaction of RSH (R = ^{t}Bu, Ph) with **1**, which is consistent with rate-limiting nucleophilic attack of RSH at the nitrido ligand followed by rapid proton transfer. On the other hand, reactions carried out in H_2O may be affected by H-bonding effects. Thus the reaction of cysteine with **1** in acidic solution exhibits a S−H/S−D isotopic effect of 2.7, and we propose a mechanism that involves both N−S bond formation and proton transfer from cysteine to a neighboring H_2O molecule in the rate-limiting step.

Our work should contribute to the understanding of the redox chemistry of nitrido complexes in aqueous solutions.

ASSOCIATED CONTENT

Supporting Information

The Supporting Information is available free of charge on the ACS Publications website at DOI: 10.1021/acs.inorgchem.8b00238.

Experimental, kinetic and spectroscopic data (PDF).

Accession Codes

CCDC 1833386 contains the supplementary crystallographic data for this paper. These data can be obtained free of charge via www.ccdc.cam.ac.uk/data_request/cif, by emailing data_

DOI: 10.1021/acs.inorgchem.8b00238
Inorg. Chem. XXXX, XXX, XXX−XXX

request@ccdc.cam.ac.uk, or by contacting The Cambridge Crystallographic Data Centre, 12 Union Road, Cambridge CB2 1EZ, UK; fax: +44 1223 336033.

AUTHOR INFORMATION

Corresponding Author

*E-mail: bhtclau@cityu.edu.hk.

ORCID

Tai-Chu Lau: 0000-0002-0867-9746

Notes

The authors declare no competing financial interest.

ACKNOWLEDGMENTS

This work was supported by the Research Grants Council of Hong Kong (CityU 9041862), Hong Kong University Grants Committee (AoE/P-03-08), and Shandong Province Natural Science Foundation (Grant ZR2017BB024).

REFERENCES

(1) Du Bois, J.; Tomooka, C. S.; Carreira, E. M. Nitridomanganese-(V) Complex: Design, Preparation, and Use as Nitrogen Atom-Transfer Reagents. *Acc. Chem. Res.* **1997**, *30*, 364−372.

(2) Eikey, R. A.; Abu-Omar, M. M. Nitrido and Imido Transition Metal Complexes of Groups 6−8. *Coord. Chem. Rev.* **2003**, *243*, 83−124.

(3) Berry, J. F. Transition Nitrido and Imido Complexes of the Late Transition Metals. *Comments Inorg. Chem.* **2009**, *30*, 28−66.

(4) Smith, J. M. Reactive Transition Metal Nitride Complexes. *Prog. Inorg. Chem.* **2014**, *58*, 417−470.

(5) Askevold, B.; Nieto, J. T.; Tussupbayev, S.; Diefenbach, M.; Herdtweck, E.; Holthausen, M. C.; Schneider, S. Ammonium Formation by Metal-Ligand Cooperative Hydrogenolysis of a Nitrido Ligand. *Nat. Chem.* **2011**, *3*, 532−537.

(6) Huynh, M. H. V.; El-Samanody, E. S.; Demadis, K. D.; Meyer, T. J.; White, P. S. Oxo-Like Reactivity of High Oxidation State Osmium Hydrazido Complexes. *J. Am. Chem. Soc.* **1999**, *121*, 1403−1404.

(7) Huynh, M. H. V.; White, P. S.; Meyer, T. J. Formation and O-Atom Reactivity of the Os(IV)-Sulfilimido and Os(IV)-Sulfoximido Complexes, cis-/trans-$[Os^{IV}(tpy)(Cl)_2(NSC_6H_3Me_2)]$ and cis-/trans-$[Os^{IV}(tpy)(Cl)_2(NS(O)C_6H_3Me_2)]$. *J. Am. Chem. Soc.* **2001**, *123*, 9170−9171.

(8) Huynh, M. H. V.; Morris, D. E.; White, P. S.; Meyer, T. J. Proton-Induced, Reversible Evolution of O_2 from the OsIV-Sulfoximido Complex $[Os^{IV}(tpy)(Cl)_2\{NS(O)\text{-}3,5\text{-}Me_2C_6H_3\}]$. *Angew. Chem., Int. Ed.* **2002**, *41*, 2330−2333.

(9) Huynh, M. H. V.; White, P. S.; Carter, C. A.; Meyer, T. J. Formation and Reactivity of the Osmium(IV)-Cyanoimido Complex $[Os^{IV}(bpy)(Cl)_3(NCN)]$. *Angew. Chem., Int. Ed.* **2001**, *40*, 3037−3039.

(10) Huynh, M. H. V.; Baker, R. T.; Jameson, D. L.; Labouriau, A.; Meyer, T. J. Formation and Reactivity of the Os(IV)-Azidoimido Complex, $PPN[Os^{IV}(bpy)(Cl)_3(N_4)]$. *J. Am. Chem. Soc.* **2002**, *124*, 4580−4582.

(11) Crevier, T. J.; Mayer, J. M. Direct Attack of Phenyl Anion at an Electrophilic Osmium-Nitrido Ligand. *J. Am. Chem. Soc.* **1998**, *120*, 5595−5596.

(12) Crevier, T. J.; Lovell, S.; Mayer, J. M. Chalcogen Atom Transfer to a Metal Nitrido. The First Transition Metal Selenonitrosyl Complex. *J. Am. Chem. Soc.* **1998**, *120*, 6607−6608.

(13) McCarthy, M. R.; Crevier, T. J.; Bennett, B.; Dehestani, A.; Mayer, J. M. Nitric Oxide Abstracts a Nitrogen Atom from an Osmium Nitrido Complex To Give Nitrous Oxide. *J. Am. Chem. Soc.* **2000**, *122*, 12391−12392.

(14) Dehestani, A.; Kaminsky, W.; Mayer, J. M. Tuning the Properties of the Osmium Nitrido Group in $TpOs(N)X_2$ by Changing the Ancillary Ligand. *Inorg. Chem.* **2003**, *42*, 605−611.

(15) Brown, S. N. Insertion of a Metal Nitride into Carbon-Carbon Double Bonds. *J. Am. Chem. Soc.* **1999**, *121*, 9752−9753.

(16) Maestri, A. G.; Cherry, K. S.; Toboni, J. J.; Brown, S. N. [4 + 1] Cycloadditions of Cyclohexadienes with Osmium Nitrides. *J. Am. Chem. Soc.* **2001**, *123*, 7459−7460.

(17) Munoz, S. B., III; Lee, W. T.; Dickie, D. A.; Scepaniak, J. J.; Subedi, D.; Pink, M.; Johnson, M. D.; Smith, J. M. Styrene Aziridination by Iron(IV) Nitrides. *Angew. Chem., Int. Ed.* **2015**, *54*, 10600−10603.

(18) Lee, W. T.; Juarez, R. A.; Scepaniak, J. J.; Munoz, S. B., III; Dickie, D. A.; Wang, H.; Smith, J. M. Reaction of an Iron(IV) Nitrido Complex with Cyclohexadienes: Cycloaddition and Hydrogen-Atom Abstraction. *Inorg. Chem.* **2014**, *53*, 8425−8430.

(19) Scepaniak, J. J.; Vogel, C. S.; Khusniyarov, M. M.; Heinemann, F. W.; Meyer, K.; Smith, J. M. Synthesis, Structure, and Reactivity of an Iron(V) Nitride. *Science* **2011**, *331*, 1049−1052.

(20) Man, W. L.; Lam, W. W. Y.; Kwong, H. K.; Yiu, S. M.; Lau, T. C. Ligand-Accelerated Activation of Strong C-H Bonds of Alkanes by a (Salen)ruthenium(VI)-Nitrido Complex. *Angew. Chem., Int. Ed.* **2012**, *51*, 9101−9104.

(21) Man, W. L.; Xie, J.; Pan, Y.; Lam, W. W. Y.; Kwong, H. K.; Ip, K. W.; Yiu, S. M.; Lau, K. C.; Lau, T. C. C−N Bond Cleavage of Anilines by a (Salen)ruthenium(VI) Nitrido Complex. *J. Am. Chem. Soc.* **2013**, *135*, 5533−5536.

(22) Man, W. L.; Lam, W. W. Y.; Yiu, S. M.; Lau, T. C.; Peng, S. M. Direct Aziridination of Alkenes by a Cationic (Salen)ruthenium(VI) Nitrido Complex. *J. Am. Chem. Soc.* **2004**, *126*, 15336−15337.

(23) Man, W. L.; Xie, J.; Lo, P. K.; Lam, W. W. Y.; Yiu, S. M.; Lau, K. C.; Lau, T. C. Functionalization of Alkynes by a (Salen)ruthenium(VI) Nitrido Complex. *Angew. Chem., Int. Ed.* **2014**, *53*, 8463−8466.

(24) Xie, J.; Man, W. L.; Wong, C. Y.; Chang, X.; Che, C. M.; Lau, T. C. Four-Electron Oxidation of Phenols to *p*-Benzoquinone Imines by a (Salen)ruthenium(VI) Nitrido Complex. *J. Am. Chem. Soc.* **2016**, *138*, 5817−5820.

(25) Arrigo, A. P. Gene Expression and the Thiol Redox State. *Free Radical Biol. Med.* **1999**, *27*, 936−944.

(26) Hand, C. E.; Honek, J. F. Biological Chemistry of Naturally Occurring Thiols of Microbial and Marine Origin. *J. Nat. Prod.* **2005**, *68*, 293−308.

(27) Moriarty-Craige, S. E.; Jones, D. P. Extracellular Thiols and Thiol/disulfide Redox in Metabolism. *Annu. Rev. Nutr.* **2004**, *24*, 481−509.

(28) Paulsen, C. E.; Carroll, K. S. Cysteine-mediated Redox Signaling: Chemistry, Biology, and Tools for Discovery. *Chem. Rev.* **2013**, *113*, 4633−4679.

(29) Jacob, C.; Giles, G. I.; Giles, N. M.; Sies, H. Sulfur and Selenium: The Role of Oxidation State in Protein Structure and Function. *Angew. Chem., Int. Ed.* **2003**, *42*, 4742−4758.

(30) Giles, N. M.; Giles, G. I.; Jacob, C. Multiple roles of cysteine in biocatalysis. *Biochem. Biophys. Res. Commun.* **2003**, *300*, 1−4.

(31) Sisley, M. J.; Jordan, R. B. Kinetic and Equilibrium Studies of the Reactions of Cysteine and Penicillamine with Aqueous Iron(III). *Inorg. Chem.* **1995**, *34*, 6015−6023.

(32) Kottapalli, K. K.; Adari, K. K.; Vani, P.; Govindan, S. K. Mechanism of Oxidation of L-cysteine by Hexachloroiridate(IV)−A Kinetic Study. *Transition Met. Chem.* **2005**, *30*, 773−777.

(33) Bridgart, G. J.; Fuller, M. W.; Wilson, I. R. Metal-ion Catalysis in Some Reactions of Hexacyanoferrate(III) Ions. Part I. Copper Catalysis in the Oxidation of Cysteine and Related Thiols. *J. Chem. Soc., Dalton Trans.* **1973**, 1274−1280.

(34) Wang, X.; Stanbury, D. M. Direct Oxidation of L-Cysteine by $[Fe^{III}(bpy)_2(CN)_2]^+$ and $[Fe^{III}(bpy)(CN)_4]^-$. *Inorg. Chem.* **2008**, *47*, 1224−1236.

(35) Hung, M.; Stanbury, D. M. Catalytic and Direct Oxidation of Cysteine by Octacyanomolybdate(V). *Inorg. Chem.* **2005**, *44*, 3541−3550.

(36) McCann, J. P.; McAuley, A. Metal-ion Oxidations in Solution. XIII. Reaction of Chromium(VI) with L-cysteine in Perchlorate Media. *J. Chem. Soc., Dalton Trans.* **1975**, 783−790.

DOI: 10.1021/acs.inorgchem.8b00238
Inorg. Chem. XXXX, XXX, XXX−XXX

(37) Shi, T.; Berglund, J.; Elding, L. I. Kinetics and Mechanism for Reduction of *trans*-Dichlorotetracyanoplatinate(IV) by Thioglycolic Acid, L-cysteine, DL-penicillamine, and Glutathione in Aqueous Solution. *Inorg. Chem.* **1996**, *35*, 3498−3503.
(38) Stevens, G. D.; Holwerda, R. A. Oxiation of Cysteine, cysteine methyl ester, and penicillamine by copper(II)-2,9-dimethyl-1,10-phenanthroline Complexes. *Inorg. Chem.* **1984**, *23*, 2777−2780.
(39) Ison, A.; Odeh, I. N.; Margerum, D. W. Kinetics and Mechanisms of Chlorine Dioxide and Chlorite Oxidations of Cysteine and Glutathione. *Inorg. Chem.* **2006**, *45*, 8768−8775.
(40) Gagliardi, C. J.; Murphy, C. F.; Binstead, R. A.; Thorp, H. H.; Meyer, T. J. Concerted Electron-Proton Transfer (EPT) in the Oxidation of Cysteine. *J. Phys. Chem. C* **2015**, *119*, 7028−7038.
(41) Man, W. L.; Lam, W. W. Y.; Kwong, H. K.; Peng, S. M.; Wong, W. T.; Lau, T. C. Reaction of a (Salen)ruthenium(VI) Nitrido Complex with Thiols. C-H Bond Activation by (Salen)ruthenium(IV) Sulfilamido Species. *Inorg. Chem.* **2010**, *49*, 73−81.
(42) Demadis, K. D.; Meyer, T. J.; White, P. S. Reactivity of Osmium(VI) Nitrides with the Azide Ion. A New Synthetic Route to Osmium(II) Polypyridyl Complexes. *Inorg. Chem.* **1998**, *37*, 3610−3619.
(43) Wang, Q.; Man, W. L.; Lam, W. W. Y.; Lau, T. C. Oxidation of Ascorbic Acid by a (Salen)ruthenium(VI) Nitrido Complex in Aqueous Solution. *Chem. Commun.* **2014**, *50*, 15799−15802.
(44) Wang, Q.; Zhao, H. Y.; Man, W. L.; Lam, W. W. Y.; Lau, K. C.; Lau, T. C. Kinetics and Mechanism of the Reaction of a Ruthenium(VI) Nitrido Complex with HSO_3^- and SO_3^{2-} in Aqueous Solution. *Chem. - Eur. J.* **2016**, *22*, 10754−10758.
(45) Man, W. L.; Tang, T. M.; Wong, T. W.; Lau, T. C.; Peng, S. M.; Wong, W. T. Highly Electrophilic (Salen)ruthenium(VI) Nitrido Complexes. *J. Am. Chem. Soc.* **2004**, *126*, 478−479.
(46) Pawlukojc, A.; Leciejewicz, J.; Ramirez-Cuesta, A. J.; Nowicka-Scheibe, J. L-Cysteine: Neutron spectroscopy, Raman, IR and ab initio study. *Spectrochim. Acta, Part A* **2005**, *61*, 2474−2481.
(47) Espenson, J. H. *Chemical Kinetics and Reaction Mechanisms*; McGraw Hill: New York, 1981.
(48) *CrysAlis*, Version 1.171.33.66; Oxford Diffraction Ltd., 2010.
(49) Sheldrick, G. M. *SHELXS-97 and SHELXL-97, Programs for Crystal Structure Solution and Refinement*; University of Göttingen: Germany, 1997.
(50) Dolomanov.; et al. Olex2, A Complete Structure Solution, Refinement and Analysis Program. *J. Appl. Crystallogr.* **2009**, *42*, 339−341.
(51) Xie, J.; Lo, P. K.; Lam, W. W. Y.; Man, W. L.; Ma, L.; Yiu, S. M.; Lau, K. C.; Lau, T. C. Oxidation of hydroquinones by a (salen)ruthenium(VI) nitride complex. *Chem. Commun.* **2016**, *52*, 11430−11433.
(52) Bicer, E.; Cetinkaya, P. A voltammetric study on the interaction of novobiocin with cysteine: pH effect. *J. Chil. Chem. Soc.* **2009**, *54*, 46−50.

DOI: 10.1021/acs.inorgchem.8b00238
Inorg. Chem. XXXX, XXX, XXX−XXX